J Mater Sci (2010) 45:4545–4553
DOI 10.1007/s10853-010-4485-5

ULTRAFINE GRAINED MATERIALS

# Unusual macroscopic shearing patterns observed in metals processed by high-pressure torsion

**Y. Cao · M. Kawasaki · Y. B. Wang · S. N. Alhajeri · X. Z. Liao · W. L. Zheng · S. P. Ringer · Y. T. Zhu · T. G. Langdon**

Received: 9 March 2010 / Accepted: 5 April 2010 / Published online: 17 April 2010


**Abstract** A duplex stainless steel was processed by high-pressure torsion (HPT) and then examined by optical microscopy. The results reveal unusual flow patterns including double-swirl strains, shear vortices, and the presence of significant local turbulence. Similar flow behavior was also visible in disks of high-purity aluminum and a Zn–22%Al eutectoid alloy. These complex flow patterns and the presence of double-swirls are consistent with the presence of a Kelvin–Helmholtz instability during HPT processing where this may arise if there are local shear velocity gradients between adjacent positions within the HPT disks.

Y. Cao · Y. B. Wang · X. Z. Liao (✉)
School of Aerospace, Mechanical and Mechatronic Engineering, The University of Sydney, Sydney, NSW 2006, Australia
e-mail: xiaozhou.liao@sydney.edu.au

M. Kawasaki · T. G. Langdon
Departments of Aerospace & Mechanical Engineering and Materials Science, University of Southern California, Los Angeles, CA 90089-1453, USA

S. N. Alhajeri · T. G. Langdon
Materials Research Group, School of Engineering Sciences, University of Southampton, Southampton SO17 1BJ, UK

W. L. Zheng
Shanghai Research Institute of Materials, 99 Handan Road, Shanghai 200437, China

S. P. Ringer
Australian Centre for Microscopy & Microanalysis, The University of Sydney, Sydney, NSW 2006, Australia

Y. T. Zhu
Department of Materials Science and Engineering, North Carolina State University, Raleigh, NC 27695-7919, USA

## Introduction

The processing of metals through the application of severe plastic deformation (SPD) has attracted much attention over the last decade because of the potential for achieving exceptional grain refinement to the submicrometer or even the nanometer level [1]. Several SPD processing techniques are now available, but most attention has centered on the procedures of equal-channel angular pressing (ECAP) [2] and high-pressure torsion (HPT) [3]. Experiments show that processing by HPT is especially effective by comparison with ECAP because it leads to smaller average grain sizes and a higher fraction of boundaries having high angles of misorientation [4, 5].

When metals are processed in HPT, there are three possible procedures as illustrated in Fig. 1 [3]. All three procedures are based on using a sample in the form of a thin disk and placing the sample between massive anvils, applying a pressure and then torsionally straining by rotating the lower anvil. Figure 1a depicts unconstrained HPT where the sample experiences only a minor back-pressure due to frictional forces so that it is free to flow outwards under the applied pressure. Figure 1b depicts constrained HPT where the sample fits into a cavity in the lower anvil and, because of the high back-pressure, there is no outward flow during torsional straining. Figure 1c depicts quasi-constrained HPT where the sample is confined within and between the two anvils but with the occurrence of some limited outward flow during processing. Early experiments were often conducted using unconstrained or constrained HPT, but more recently most experiments are conducted using quasi-constrained HPT [3].

An important requirement in processing by HPT is to estimate the strain imposed on the sample. Using a

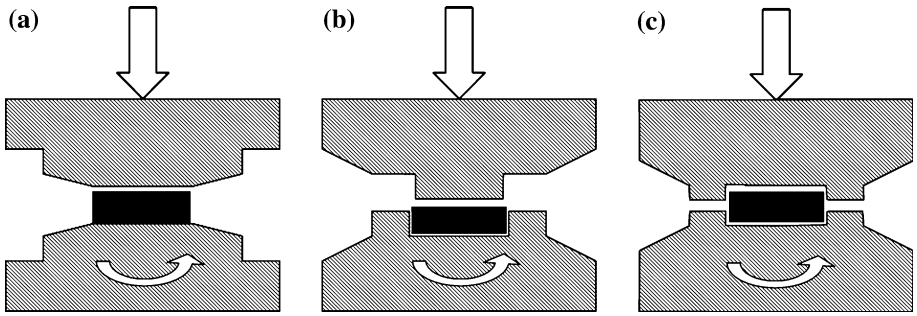


**Fig. 1** Schematic illustration of HPT for **a** unconstrained, **b** constrained, and **c** quasi-constrained conditions [3]

rigid-body analysis, and neglecting the relatively minor strain incurred in the sample from the applied pressure, the equivalent von Mises strain, $\varepsilon_{eq}$, imposed on the disk in torsional straining is given by [6–8]

$$\varepsilon_{eq} = \frac{2\pi Nr}{h\sqrt{3}} \quad (1)$$

where $N$ is the number of revolutions, $r$ is the distance from the center of the disk, and $h$ is the disk height (or thickness). Several basic conclusions arise from this simple rigid-body analysis. First, for any disk the imposed shear strain, and therefore the measured hardness, is dependent only upon the radial distance from the center of the disk. Second, the direction of shear straining at any position within the disk is perpendicular to the radial direction at that point. Third, the shear strain at the center of the disk is zero.

Although these calculations suggest the occurrence of high hardness and significant grain refinement around the edges of disks processed by HPT with low hardness and little or no grain refinement in the center, early experiments revealed a microstructural evolution with increasing strain so that the structure gradually became reasonably homogeneous [9]. This evolution was explained in terms of a model in which the internal deformation within the disk develops in an undulating manner in the outer ring of the disk and then spreads inwards to the center [10]. The development of homogeneous structures in HPT was later further developed using strain gradient plasticity and incorporating a microstructure-related constitutive description of the material behavior [11]. This evolution with strain is not consistent with the conventional rigid-body analysis inherent in the derivation of Eq. 1, and it demonstrates instead that the flow characteristics in HPT processing are more complex and interrelated than may be accommodated within a simple mathematical analysis.

The contradictions with conventional analyses were further confirmed in very recent observations of unusual shearing patterns that are visible on a macroscopic scale on disks processed by HPT [12]. Accordingly, the objective of this article is to examine these recent observations and to describe additional results that confirm the presence of unusual flow behavior when processing by HPT

## Experimental materials and procedures

The results in this report are based on experiments described earlier and conducted using a duplex stainless steel [12], the Zn–22%Al eutectoid alloy [13], and high-purity (99.99%) aluminum [14]: the steel was a commercial DP3W super duplex stainless steel containing, in wt%, C 0.017, Si 0.3, Mn 0.5, P 0.015, S 0.001, Ni 7.0, Cr 25, Mo 3.3, W 2.0, and N 0.28. Full details of the materials and the various processing conditions were given earlier, and therefore, it is necessary to provide only limited information.

All materials were prepared in the form of thin disks having diameters of ~10 mm and thicknesses of ~0.8 mm. They were all processed under quasi-constrained HPT conditions as illustrated in Fig. 1c using different applied pressures, rotation speeds of either 1 or 1/4 rpm, and torsional straining from 1 to 16 revolutions. Following HPT, all disks were mechanically polished and etched for optical examination. Using X-ray diffraction, no phase transformations were detected in the stainless steel after HPT. Furthermore, the absence of any phase transformation was also evident in the earlier report using transmission electron microscopy [12].

## Experimental results

### Stainless steel

Figure 2 shows the microstructure within the as-received material. There are lighter-contrast austenitic ($\gamma$) phase islands aligned essentially in the same direction and lying within a darker-contrast ferritic ($\alpha$) phase matrix. These two phases have similar volume fractions and exhibit good contrast so that they provide a good capability for revealing the shear strains imposed in HPT.

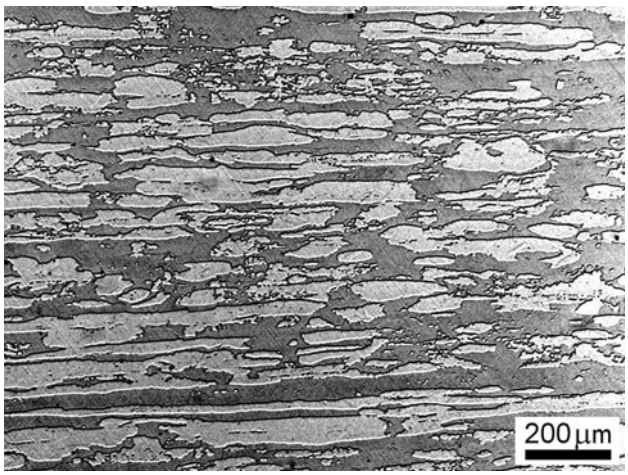


**Fig. 2** A typical microstructure of the as-received duplex stainless steel; the lighter-contrast austenitic ($\gamma$) phase islands are merged within the darker-contrast ferritic ($\alpha$) phase matrix

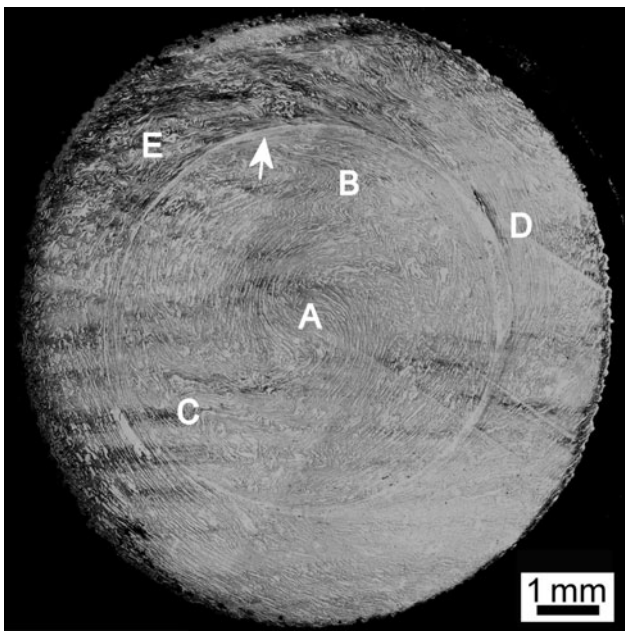


**Fig. 3** Optical micrograph of a disk of the stainless steel processed for 5 revolutions using a pressure of 6.0 GPa: the *white arrow* indicates a ring of strain positioned on the center of the disk at A and the points labeled B to E are examined in detail in the following figures [12]

A representative disk is shown in Fig. 3 after experiencing 5 revolutions under an applied pressure of 6.0 GPa at a speed of 1 rpm [12]. The white arrow delineates a well-defined ring that is accurately positioned on the center of the disk at A. This ring corresponds closely to the anticipated behavior under a rigid-body situation such that the strain is dependent upon the radial distance from the center of the disk and the direction of straining is perpendicular to the radial direction. The points

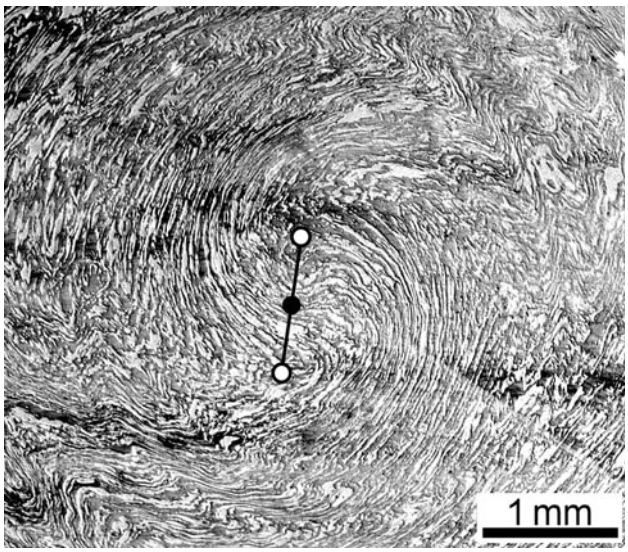


**Fig. 4** An optical micrograph at the center A of the disk shown in Fig. 3: a unique double-swirl pattern is observed where the two *white circles* correspond to the two centers of the double-swirls and the *solid circle* corresponds to the center of the disk

labeled B to E are examined in detail in the following paragraphs.

Figure 4 shows the flow pattern in the vicinity of the center of the disk at A [12]. This micrograph contains a unique double-swirl pattern where the two open points correspond to the centers of the two swirls and the closed point is located at the center of the disk. It is apparent that the microstructure between the two swirls in the vicinity of the center of the disk is extended in a direction consistent with the swirling pattern, thereby confirming that the shear strain is nonzero at the center. This illustration provides unambiguous evidence for a deviation from the rigid-body analysis when processing by HPT. Furthermore, it is important to note this deviation is present despite the well-defined ring shown by the white arrow in Fig. 3 which appears to be consistent with the conventional analysis. Detailed observations showed these double-swirl patterns were present in all disks processed for at least 3 revolutions when using an applied pressure of 6.0 GPa. Furthermore, it was found that the measured distance between the centers of the two swirls, given by the length of the line in Fig. 4, decreased with increasing numbers of revolutions.

The optical micrograph in Fig. 5 was taken at the point labeled B in Fig. 3, and it corresponds essentially to one of the two tails of the double-swirl pattern: the white arrow indicates the radial direction from the center to the circumference. Within this tail, it is apparent that the shear strain direction lies approximately parallel to the radial direction. Furthermore, both tails of the double-swirl appeared reasonably symmetric with respect to the center of the disk.

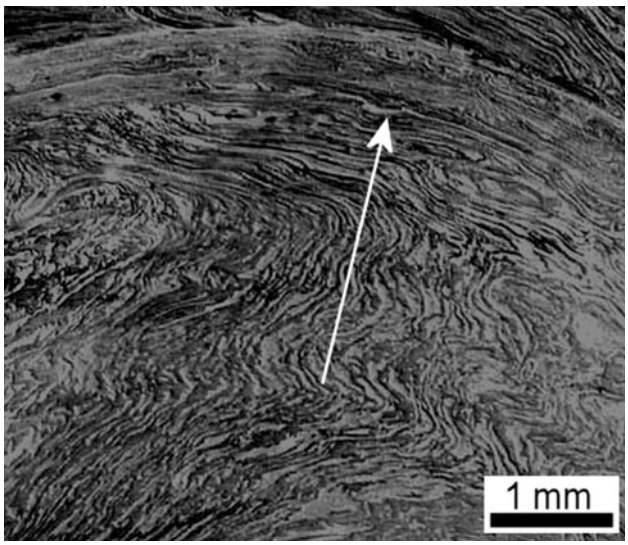


**Fig. 5** Optical micrograph of the tail of a double-swirl at the position labeled B in Fig. 3: the *white arrow* indicates the radial direction from the center to the circumference

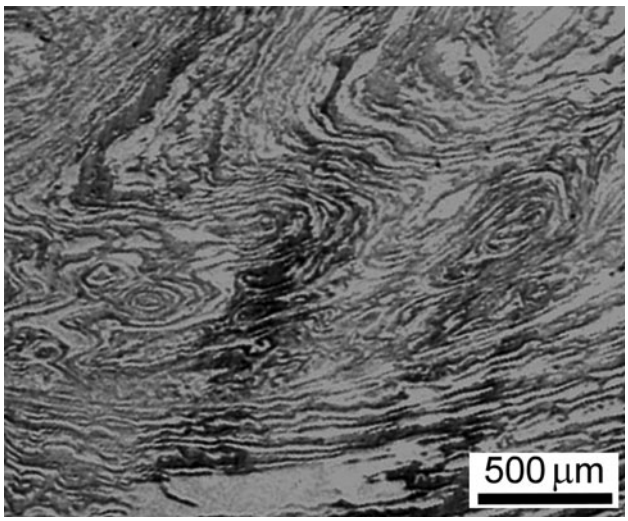


**Fig. 6** Optical micrograph showing local shear vortices at the position labeled C in Fig. 3

Figure 6 shows a magnified view at position C in Fig. 3 where there is significant turbulence with well-defined local shear vortices containing phase domains. These domains are extended more severely and indicate the presence of higher shear strains in the vicinity of each vortex. It was found that these shear vortices are relatively common in duplex stainless steel disks processed through low numbers of revolutions but they gradually disappear as the number of revolutions increases.

Closer to the edge of the disk, Fig. 7 shows optical micrographs recorded from Fig. 3 where Fig. 7a corresponds to point D and Fig. 7b corresponds to point E.

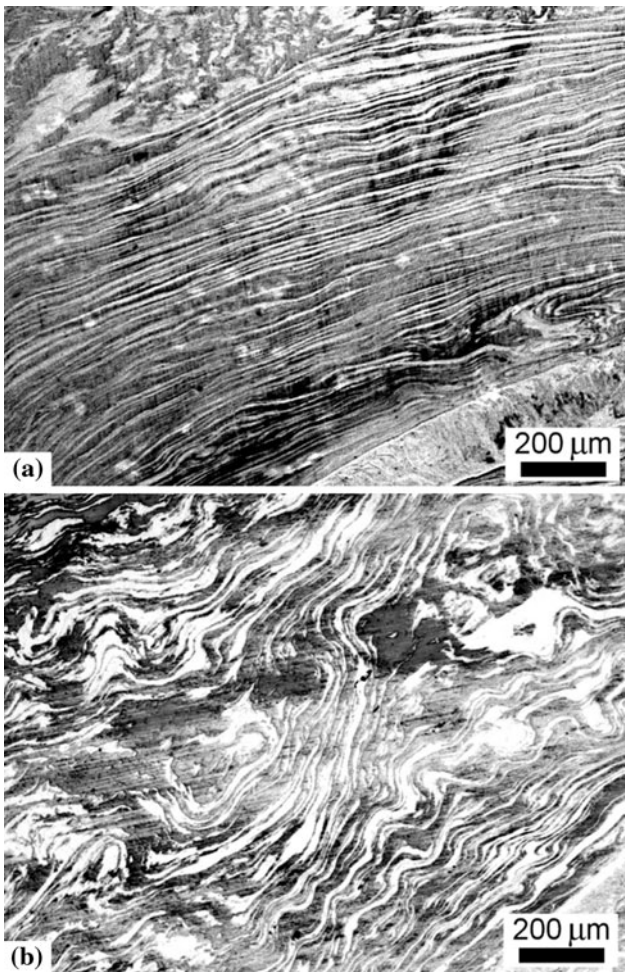


**Fig. 7** Optical micrographs showing the microstructures close to the edge of the disk in Fig. 3: **a** shows a regular strain morphology at the position labeled D and **b** shows local turbulence at the position labeled E

In Fig. 7a the flow lines are regular, equally spaced, and reasonably parallel to the circumference of the disk, thereby demonstrating near-perfect shear straining within this region. By contrast, in Fig. 7b there is gross turbulence and the flow patterns are irregular and delineate many local vortices. Although the overall impression in Fig. 7b is that the shear strains are approximately parallel to the disk circumference, on a local level there is much shear turbulence and highly irregular flow patterns. It is important to note that positions D and E in Fig. 7a and b have essentially the same radial distance of $\sim$3.5 mm from the center of the disk. These observations show, therefore, that processing by 5 revolutions is not sufficient in this material to achieve the same level of straining at all positions in the disk having the same radial values.

An earlier report showed a regular double-swirl about the center of a disk processed through 20 revolutions of HPT under a pressure of 4.0 GPa [12], and a similar

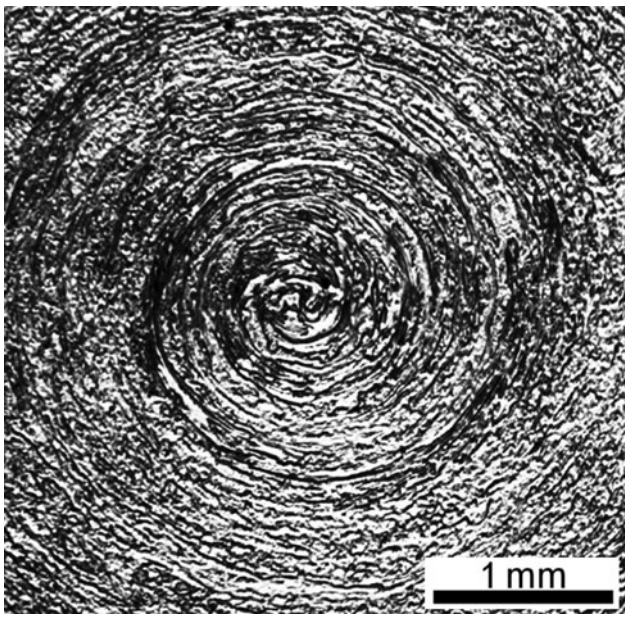


**Fig. 8** Optical micrograph of the center of a disk processed for 16 revolutions using a pressure of 8.0 GPa

illustration is shown in Fig. 8 for a sample processed through 16 revolutions with a pressure of 8.0 GPa and a speed of 1 rpm. Under these conditions of a high applied pressure and a large number of revolutions, the double-swirl has essentially evolved into a single swirl which is now positioned on the center of the disk. There is now very little evidence for the swirl tails although they were clearly visible in Fig. 5 after 5 revolutions at 6.0 GPa. Furthermore, the local shear vortices evident after 5 revolutions in Figs. 6 and 7b are now absent and the direction of the imposed shear strain is consistent with the anticipated behavior from the rigid-body analysis. The absence of shear vortices shows there are no longer any significant local variations in the shear strains. This is consistent with hardness measurements on a number of materials which show that at high pressure and large numbers of revolutions there is an essentially homogeneous structure [15–18].

## Zn–22%Al eutectoid alloy

The duplex stainless steel described in the preceding section is an excellent material for these observations because of the presence of two discrete and well-defined phases having approximately equal fractions. However, there is evidence also for comparable flow patterns in the Zn–22%Al eutectoid alloy where the binary microstructure contains an Al-rich ($\alpha$) phase and a Zn-rich ($\beta$) phase and the two phases appear in the photomicrographs as black and white areas, respectively. The initial microstructure in this alloy contained both equiaxed regions with an average grain size of $\sim$1.4 μm and a lamellar structure consisting of thin layers of alternating $\alpha$ and $\beta$ phases having average thicknesses of $\sim$100 nm.

Figure 9 shows the microstructures observed at (a) the edge and (b) the center of a disk processed by HPT through 1 revolution at a pressure of 3.0 GPa using the reduced speed of 1/4 rpm [13]. Measurements showed that the grains were refined by HPT to an average size of $\sim$450 nm near the edge of the disk and, in addition, the grains were no longer distributed homogeneously but rather they lay in agglomerates which delineated the flow of torsional straining around the periphery of the disk. The development of agglomerates in processing by HPT was also noted in very early experiments on this alloy [19]. Thus, as with the duplex stainless steel, the microstructure is again aligned along the direction of shear at the outer edge of the disk. By contrast, at the center of the disk there were regions of both equiaxed grains with an average size of $\sim$500 nm and a lamellar structure with average layer widths of $\sim$100 nm. The reduction in grain size from $\sim$1.4 μm to $\sim$500 nm in the central region again confirms that the shear strain in the center of the disk is nonzero. It was determined by careful analysis that the alignment of the Zn and Al agglomerates with the torsional flow lines was restricted to a width of $<$ 1 mm from the edge of the disk.

Figure 10 shows the variation in the microstructure at the edge (on the left) and at the center (on the right) of

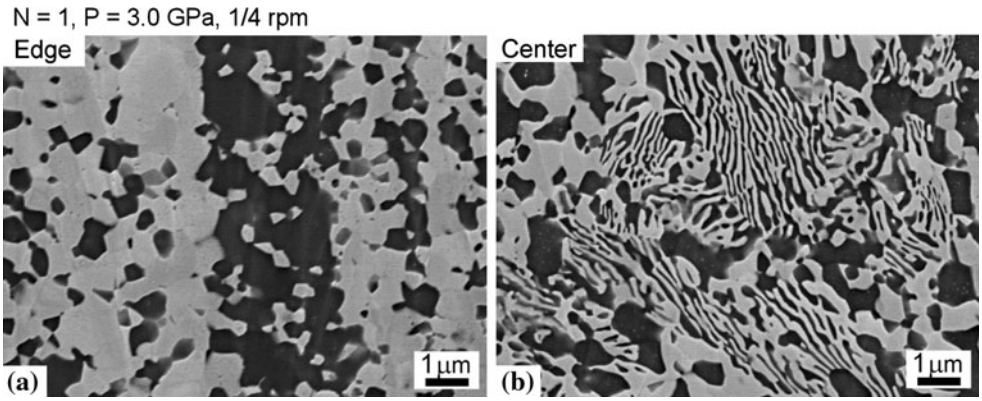


**Fig. 9** Micrographs taken on the Zn–22%Al eutectoid alloy disk processed by HPT for 1 turn at a pressure of 3.0 GPa using a speed of 1/4 rpm: **a** near the edge of the disk and **b** near the center of the disk [13]

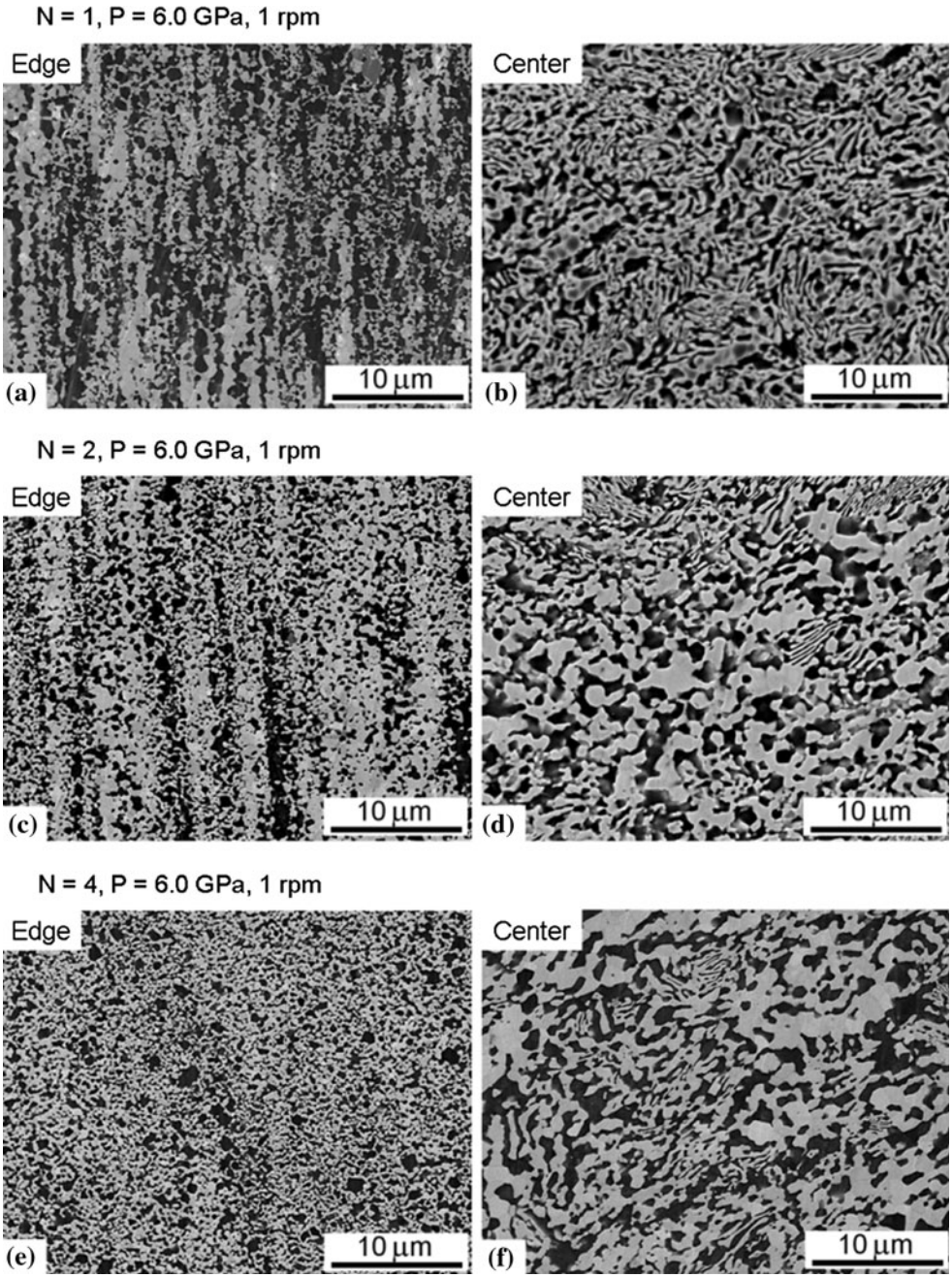


**Fig. 10** Representative micrographs of the Zn–22%Al eutectoid alloy taken after different processing conditions where the *left column* corresponds to microstructures taken at positions near the edges of the disks and the *right column* shows regions near the centers [13]

disks processed with an applied pressure of 6.0 GPa using a speed of 1 rpm through 1 turn (upper row), 2 turns (middle row), and 4 turns (lower row), respectively. These photomicrographs demonstrate an evolution in structure with increasing number of turns in HPT such that the evidence for banding and alignment near the edge of the disk essentially disappears after 4 turns in Fig. 10e. Measurements showed the grain sizes near the edges were reduced to ~350 nm after 2 and 4 turns whereas in the center of the disk taken through 4 revolutions the equiaxed grain size was ~700 nm and the average lamellar width was ~200 nm.

High-purity aluminum

The high-purity aluminum had an initial grain size of ~1 mm, and it was processed by HPT under both monotonic and cyclic conditions using an applied pressure of 6.0 GPa and a speed of 1 rpm. For the cyclic tests, the direction of torsional straining was changed within <2 s.

Figure 11 shows an optical micrograph after HPT through 1 revolution where the central region of the disk in Fig. 11a is presented in a magnified form in the lower image in Fig. 11b [14]. Careful inspection shows that, again as in the duplex stainless steel, the microstructure

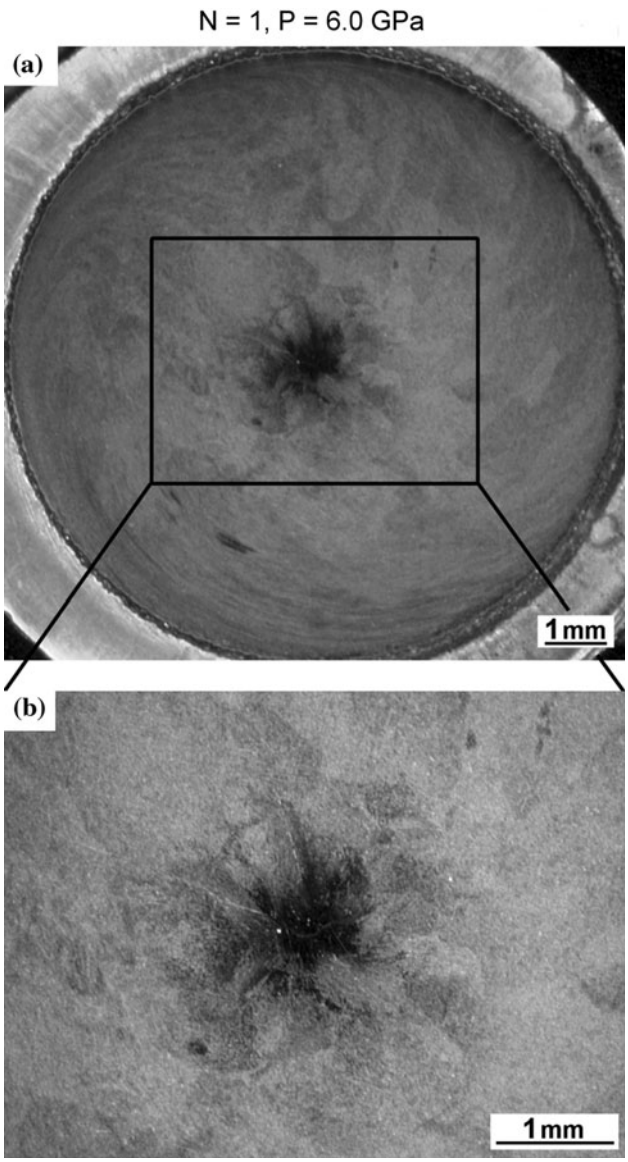


**Fig. 11** **a** Optical micrograph showing the polished and etched surface of a pure aluminum disk processed by HPT for 1 turn using a pressure of 6.0 GPa and **b** the magnified appearance of the central region of the disk [14]

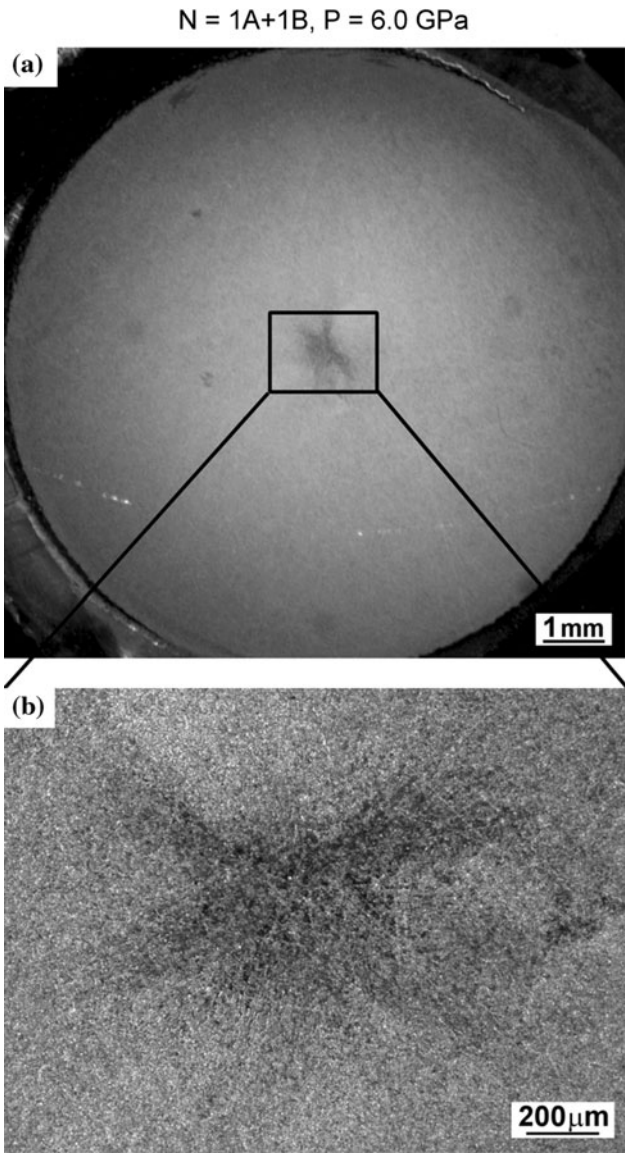


**Fig. 12** **a** Optical micrograph showing the polished and etched surface of a pure aluminum disk processed by HPT through one forward turn (1A) and one reverse turn (1B) using a pressure of 6.0 GPa and **b** the magnified appearance of the central region of the disk [14]

tends to be extended in the direction of straining near the edge of the disk and in the center there is evidence for the development of a swirl pattern. Although the pattern in the disk center is less clearly resolved in the high-purity aluminum because of the absence of a two-phase structure, the results nevertheless suggest that the development of swirls is a characteristic feature of materials processed by HPT.

Finally, Fig. 12 demonstrates the use of cyclic testing where the direction of torsional straining was reversed and there was 1 turn in the forward (A) direction and 1 turn in the backward (B) direction. The two images again show the whole disk in Fig. 12a and the central region in Fig. 12b but for this cyclic condition there is no clear evidence for the development of a swirl. This suggests that a reversal in the straining direction may tend to cancel any swirling that is initially introduced when processing in the forward direction.

## Discussion

Observations on disks of a duplex stainless steel processed by HPT through at least three revolutions have revealed unusual shearing patterns in the form of double-swirls, formed around the center of each disk, with the presence of

much turbulence and many local shear vortices. These patterns are not due to slippage of the disk within the HPT facility because care was exercised to ensure there was no slippage during the processing [20] and, in addition, slippage will not produce symmetrical patterns as in the double-swirls. These unusual results are also matched by observations on high-purity aluminum and a Zn–22%Al eutectoid alloy. The generality of these observations suggests that the formation of a complex shear patterning is a characteristic feature of the processing of disks by HPT. Although these effects were not incorporated directly into the strain gradient plasticity modeling developed recently to explain the gradual evolution of homogeneity in disks processed by HPT [11], the effect is included indirectly through the reaction stresses that are incorporated in the model to account for the plastic strain incompatibilities between adjacent grains.

It is interesting to note that vortex microstructures have been reported in other areas of materials science including in the weld zones after friction stir welding [21] and in the shear patterns of metals deformed at very rapid strain rates [22]. It is well known that local vortices occur in continuous fluids having velocity variations and in situations where there are two fluids having a sufficient velocity difference across their mutual interface. These differences give rise to the Kelvin–Helmholtz instability which is a well-established phenomenon in many areas of physics including in fluid flow [23–25], in plasma physics [26–28], in atmospheric physics [29, 30], and in oceanography [31]. Although the present observations on HPT disks require additional experiments to provide a complete understanding of the nature of the flow processes in HPT, it appears nevertheless that there are local shear velocity differences between adjacent positions within the HPT disks and this leads, at 3 or more revolutions of HPT, to local vortices and gross turbulence which spread over wide areas.

It is readily apparent from these observations that Eq. 1, which derives directly from a rigid-body analysis, is not strictly followed in processing by HPT and instead there are local variations and protuberances within the flow patterns which occur at all positions within the HPT disks. This suggests that a better representation of microstructural evolution may be attained at the local scale by using the strain gradient plasticity model. Nevertheless, it was demonstrated in very early experiments on HPT that hardness measurements recorded across the disk diameters may be correlated directly by plotting the individual hardness values against the equivalent strain calculated from Eq. 1 [32]. Furthermore, the approach of plotting hardness against equivalent strain has been used successfully in numerous subsequent HPT experiments [17, 18, 33, 34]. The success of this approach suggests that the vortices and turbulence visible in the macroscopic images in this report are restricted primarily to local perturbations so that, when considering strains over a much longer length scale, the rigid-body analysis and Eq. 1 remains a reasonable representation of the strain introduced in HPT.

## Summary and conclusions

1. Experiments on a duplex stainless steel processed by HPT reveal unusual flow patterns including double-swirl strains, shear vortices, and the presence of significant local turbulence. These results are supported by observations on high-purity aluminum and a Zn–22%Al eutectoid alloy.

2. The results show that, at the local level, there is a significant deviation from the rigid-body analysis which is generally used to estimate the strain in HPT. The complex flow patterns and the presence of double-swirls observed after HPT are consistent with a Kelvin–Helmholtz instability which may arise if there are local shear velocity gradients between adjacent positions within the HPT disks.

**Acknowledgements** The authors express their great appreciation to the scientific and technical input and support from the Australian Microscopy & Microanalysis Research Facility node at the University of Sydney. This project was supported by the Australian Research Council [Grant No. DP0772880 (Y.C., Y.B.W., and X.Z.L.)], the U.S. DOE IPP program (Y.T.Z.), and the National Science Foundation of the United States [Grant No. DMR-0855009 (M.K. and T.G.L.)].

## References

1. Valiev RZ, Islamgaliev RK, Alexandrov IV (2000) Prog Mater Sci 45:103
2. Valiev RZ, Langdon TG (2006) Prog Mater Sci 51:881
3. Zhilyaev AP, Langdon TG (2008) Prog Mater Sci 53:893
4. Zhilyaev AP, Kim BK, Nurislamova GV, Baró MD, Szpunar JA, Langdon TG (2002) Scr Mater 48:575
5. Zhilyaev AP, Kim BK, Szpunar JA, Baró MD, Langdon TG (2005) Mater Sci Eng A391:377
6. Valiev RZ, Ivanisenko YuV, Rauch EF, Baudelet B (1996) Acta Mater 44:4705
7. Wetscher F, Vorhauer A, Stock R, Pippan R (2004) Mater Sci Eng A387–389:809
8. Wetscher F, Pippan R, Sturm S, Kauffmann F, Scheu C, Dehm G (2006) Metall Mater Trans 37A:1963
9. Zhilyaev AP, Lee S, Nurislamova GV, Valiev RZ, Langdon TG (2001) Scr Mater 44:2753
10. Zhilyaev AP, Nurislamova GV, Kim BK, Baró MD, Szpunar JA, Langdon TG (2003) Acta Mater 51:753
11. Estrin Y, Molotnikov A, Davies CHJ, Lapovok R (2008) J Mech Phys Solids 56:1186
12. Cao Y, Wang YB, Alhajeri SN, Liao XZ, Zheng WL, Ringer SP, Langdon TG, Zhu YT (2010) J Mater Sci 45:765. doi: 10.1007/s10853-009-3998-2
13. Kawasaki M, Ahn B, Langdon TG (2010) Acta Mater 58:919
14. Kawasaki M, Langdon TG (2008) Mater Sci Eng A498:341
15. Xu C, Horita Z, Langdon TG (2007) Acta Mater 55:203
16. Xu C, Horita Z, Langdon TG (2008) Acta Mater 56:5168
17. Edalati K, Fujioka T, Horita Z (2008) Mater Sci Eng A497:168

18. Ito Y, Horita Z (2009) Mater Sci Eng A503:32
19. Furukawa M, Ma Y, Horita Z, Nemoto M, Valiev RZ, Langdon TG (1998) Mater Sci Eng A241:122
20. Edalati K, Horita Z, Langdon TG (2009) Scr Mater 60:9
21. Zhang HW, Zhang Z, Chen JT (2007) J Mater Process Technol 183:62
22. Guduru PR, Ravichandran G, Rosakis AJ (2001) Phys Rev E 64:036128
23. Rangel RH, Sirignano WA (1988) Phys Fluids 31:1845
24. Fernando HJS (1991) Ann Rev Fluid Mech 23:455
25. Funada T, Joseph DD (2001) J Fluid Mech 445:263
26. Nakamura TKM, Fujimoto M (2008) Phys Rev Lett 101:165002
27. Wright S, Presura R, Esaulov A, Neff S, Plechaty C, Martinez D, Haboub A (2009) Astrophys Space Sci 322:201
28. Yamamoto T (2009) J Geophys Res 114:A06207
29. De Silva IPD, Fernando HJS, Eaton F, Hebert D (1996) Earth Planet Sci Lett 143:207
30. Plant RS, Keith GJ (2007) Boundary-Layer Meterol 122:1
31. van Haren H, Gostiaux L (2010) Geophys Res Lett 37:L03605
32. Vorhauer A, Pippan R (2004) Scr Mater 51:921
33. Edalati K, Fujioka T, Horita Z (2009) Mater Trans 50:44
34. Xu C, Horita Z, Langdon TG (2010) Mater Trans 51:2